CHEMISTRY
A EUROPEAN JOURNAL

DOI: 10.1002/chem.200501027

Infrared-Spectroscopic and Density-Functional-Theory Investigations of the LaCO, $La_2[\eta^2(\mu_2\text{-C,O})]$, and *c*-$La_2(\mu\text{-C})(\mu\text{-O})$ Molecules in Solid Argon

Qiang Xu,* Ling Jiang, and Ru-Qiang Zou[a]

Abstract: Reactions of laser-ablated lanthanum atoms with CO molecules in solid argon have been studied. The neutral lanthanum monocarbonyl (LaCO), produced upon sample deposition at 7 K, exhibits a C–O stretching frequency of 1772.7 cm^{-1}; to the best of our knowledge this is the lowest yet observed for a terminal CO in a neutral metal–carbonyl molecule (MCO, M = metal atom), implying anomalously enhanced metal-to-CO back-bonding. The infrared (IR) absorption band at 1145.9 cm^{-1} is assigned to the C–O stretching mode of the side-on-bonding CO in the $La_2[\eta^2(\mu_2\text{-C,O})]$ molecule. This CO-activated molecule undergoes an UV/Vis-photoinduced rearrangement to the CO-dissociated molecule, *c*-$La_2(\mu\text{-C})(\mu\text{-O})$. Density functional theory (DFT) calculations have been performed on these molecules, the results of which lend strong support to the experimental assignments of the IR spectra. LaCO is predicted to have a quartet ground state, corresponding to a linear geometry. Its formation involves La 6s→4f promotion, which increases the strength of La–CO bonding by decreasing the σ repulsion and, remarkably, by increasing the La 5d and 4f→CO 2π back-bonding. The observations schematically depict the whole process, starting with the interaction of CO with metal and ending with CO dissociation by the lanthanum dimer.

Keywords: density functional calculations · IR spectroscopy · lanthanum · matrix isolation

Introduction

The study of the reactions of carbon monoxide with metal atoms is a topic of considerable academic and industrial interest.[1] In particular, metal monocarbonyls (MCOs, M = metal) are often considered as prototypes for CO chemisorption on metal surfaces.[2] The C–O stretching frequency ν_{C-O} of a terminal CO moiety in a neutral MCO molecule is typically in the 2050–1810 cm^{-1} range.[3] Remarkably, the thorium carbonyl complex ThCO, generated from the reactions of laser-ablated Th with CO molecules in excess neon, exhibits a very large metal-to-CO π-back-donation, as indicated by $\nu_{C-O} = 1817.5\ cm^{-1}$.[4] CO activation by transition metals is a matter of great importance in a large number of industrial processes.[5] Very recently, we employed IR spectroscopy and DFT studies to characterize the $Sc_2[\eta^2(\mu_2\text{-C,O})]$ molecule, an unprecedented homoleptic dinuclear metal carbonyl compound with an asymmetrically bridging and side-on-bonding CO moiety. We found that this CO-activated molecule undergoes UV/Vis-photoinduced rearrangement to the CO-dissociated molecule, *c*-$Sc_2(\mu\text{-C})(\mu\text{-O})$.[6]

Recent studies have shown that with the aid of isotopic substitution techniques, a combination of matrix-isolation IR spectroscopy and quantum chemical calculations can be a very powerful tool for the investigation of the IR spectra, structure, and bonding of novel species.[3,4,6,7] In contrast to extensive experimental and theoretical studies of the interactions of CO molecules with the transition metals and the main-group elements, there is very little known about the lanthanum carbonyl molecule. Previous calculations predicted a preference for the CO molecule to coordinate to lanthanum through the carbon atom to form the linear metal carbonyl compound.[8] Here we report a study of reactions of laser-ablated lanthanum atoms with carbon monoxide in excess argon. We will show that the neutral lanthanum monocarbonyl LaCO with its unusually low C–O stretching frequency (implying an anomalously enhanced metal-to-CO

[a] Prof. Dr. Q. Xu, L. Jiang, R.-Q. Zou
National Institute of Advanced Industrial Science and Technology (AIST)
Ikeda, Osaka 563-8577 (Japan)
and
Graduate School of Science and Technology
Kobe University, Nada Ku, Kobe
Hyogo 657-8501 (Japan)
Fax: (+81) 72-751-9629
E-mail: q.xu@aist.go.jp

back-donation) is formed upon sample deposition and the intensity of which increased on annealing. UV/Vis-photoinduced rearrangement of $La_2[\eta^2(\mu_2\text{-C,O})]$ to $c\text{-}La_2(\mu\text{-C})(\mu\text{-O})$ is also observed. DFT calculations were performed to confirm the experimental findings and corroborate spectral assignments. These calculations also facilitated the prediction of the structures of the reaction products and the elucidation of the electron configuration and bonding characteristics of the key molecule LaCO.

Experimental Section

The experimental procedures for laser ablation and matrix-isolation IR spectroscopy employed here have been described in detail previously.[9,10] In the experiment the Nd:YAG laser fundamental (1064 nm, 10 Hz repetition rate with 10 ns pulse width) was focused on a rotating La target. The laser-ablated La atoms were codeposited with CO in excess argon onto a CsI window, cooled to 7 K by means of a closed-cycle helium refrigerator. A laser power of 4–9 mJ per pulse was typically used. Carbon monoxide (99.95% CO), $^{13}C^{16}O$ (99%, $^{18}O < 1\%$), and $^{12}C^{18}O$ (99%) were used in the preparation of the CO/Ar mixtures. Matrix samples were deposited for one to two hours with a typical rate of 2–4 mmol per hour. Following sample deposition, IR spectra were recorded on a BIO-RAD FTS-6000e spectrometer at 0.5 cm^{-1} resolution using a liquid-nitrogen cooled HgCdTe (MCT) detector for the 5000–400 cm^{-1} spectral range. Samples were annealed at different temperatures and subjected to broad-band irradiation ($\lambda > 250$ nm) using a high-pressure mercury-arc lamp (Ushio, 100 W).

Computational methods: Quantum-chemical calculations, to predict the structures and vibrational frequencies of the observed reaction products, were performed using the Gaussian 03 program.[11] The BPW91 density functional was used.[12] The 6–311++G(d,p) basis sets were used for C and O atoms, and the SDD pseudopotential for La atoms.[13] Geometries were fully optimized and vibrational frequencies were calculated with analytical second derivatives. The natural-bond-orbital (NBO)[14] approach was employed in the analysis of the electron configuration and the bonding characteristics of the LaCO molecule.

Results and Discussion

Experiments were performed with carbon monoxide concentrations ranging from 0.02% to 0.2% in excess argon. Typical IR spectra for the reactions of laser-ablated La atoms with CO molecules in excess argon are illustrated in Figures 1–4, and the absorption bands in different isotopic experiments are listed in Table 1. The stepwise-annealing and photolysis behaviors of the product IR absorption bands are also shown in the figures and will be discussed below. Experiments employing the electron scavenger CCl_4, doped at various concentrations in solid argon, were also undertaken.

Quantum-chemical calculations were carried out for all possible isomers of the potential product molecules. Figure 5 shows representative optimized structures of the reaction products. Molecular-orbital pictures of the quartet ground state of LaCO, showing the highest occupied molecular orbitals down to the third valence molecular orbital from the HOMO, are plotted in Figure 6. Table 2 provides a comparison of the observed and calculated isotopic frequencies for

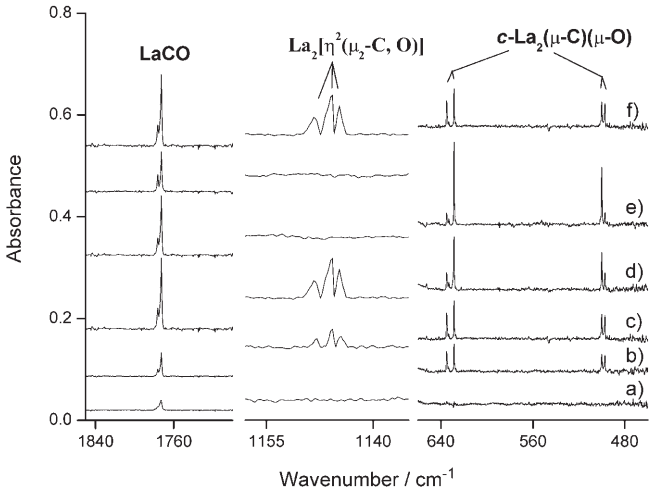

Figure 1. IR spectra in the 1850–1700, 1160–1130, and 650–460 cm^{-1} ranges for laser-ablated La atoms co-deposited with 0.02% CO in Ar at 7 K. a) After 60 min of sample deposition, b) after annealing to 30 K, c) after annealing to 34 K, d) after 20 min of broad-band irradiation, e) after annealing to 36 K, and f) doped with 0.005% CCl_4, after annealing to 34 K.

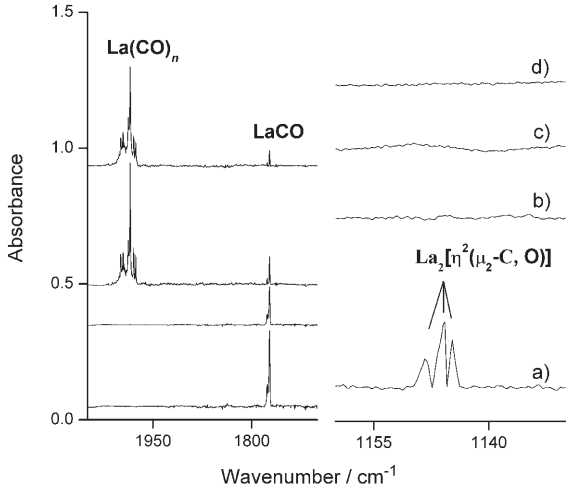

Figure 2. IR spectra in the 2100–1700 cm^{-1} and 1160–1130 cm^{-1} ranges for laser-ablated La atoms co-deposited with different CO concentrations and different laser powers in Ar, after annealing to 34 K. a) 0.02% CO, 9 mJ per pulse, b) 0.02% CO, 4 mJ per pulse, c) 0.06% CO, 4 mJ per pulse, and d) 0.2% CO, 4 mJ per pulse.

the reaction products. The results of the NBO analysis for the LaCO molecule are presented in Table 3. The natural electron configuration of the LaCO molecule is listed in Table 4.

LaCO: The major feature in the C–O stretching region at 1772.7 cm^{-1}, with one trapping site at 1776.3 cm^{-1} (Table 1 and Figure 1), was observed after sample deposition. The intensities of these bands sharply increase on annealing, withstand broad-band irradiation, and slightly decrease on further annealing. The main band at 1772.7 cm^{-1} shifts to

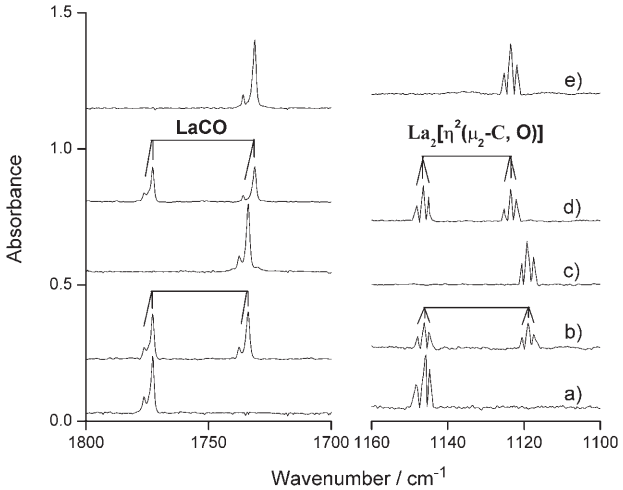

Figure 3. IR spectra in the 1800–1700 cm^{-1} and 1160–1100 cm^{-1} ranges for laser-ablated La atoms co-deposited with isotopic CO in Ar for 60 min at 7 K, followed by annealing to 34 K. a) 0.02 % $^{12}C^{16}O$, b) 0.01 % $^{12}C^{16}O$ + 0.01 % $^{13}C^{16}O$, c) 0.02 % $^{13}C^{16}O$, d) 0.01 % $^{12}C^{16}O$ + 0.01 % $^{12}C^{18}O$, and e) 0.02 % $^{12}C^{18}O$.

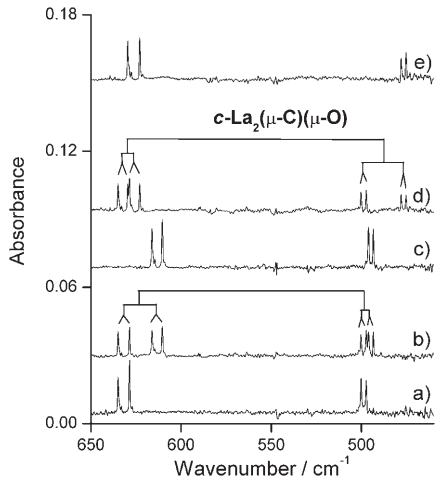

Figure 4. IR spectra in the 650–460 cm^{-1} range for laser-ablated La atoms codeposited with isotopic CO in Ar for 60 min at 7 K, followed by annealing to 34 K and broad-band irradiation for 20 min. a) 0.02 % $^{12}C^{16}O$, b) 0.01 % $^{12}C^{16}O$ + 0.01 % $^{13}C^{16}O$, c) 0.02 % $^{13}C^{16}O$, d) 0.01 % $^{12}C^{16}O$ + 0.01 % $^{12}C^{18}O$, and e) 0.02 % $^{12}C^{18}O$.

Table 1. IR absorptions [cm^{-1}] observed after codeposition of laser-ablated La atoms with CO in excess argon at 7 K.

$^{12}C^{16}O$	$^{13}C^{16}O$	$^{12}C^{18}O$	$^{12}C^{16}O$ + $^{13}C^{16}O$	$^{12}C^{16}O$ + $^{12}C^{18}O$	$^{12}C/^{13}C$	$^{16}O/^{18}O$	Assignment
1985.0	1942.3	1937.5			1.0220	1.0245	$La(CO)_n$
1776.3	1737.6	1735.9	1776.3, 1737.6	1776.3, 1735.9	1.0223	1.0233	LaCO site
1772.7	1733.8	1731.1	1772.7, 1733.7	1772.7, 1731.1	1.0224	1.0240	LaCO
1147.9	1120.5	1125.2	1147.9, 1120.5	1147.9, 1125.2	1.0245	1.0202	$La_2[\eta^2(\mu_2\text{-C,O})]$ site
1145.9	1118.5	1123.2	1145.9, 1118.5	1145.9, 1123.2	1.0245	1.0202	$La_2[\eta^2(\mu_2\text{-C,O})]$
1144.9	1117.5	1122.2	1144.9, 1117.5	1144.9, 1122.2	1.0245	1.0202	$La_2[\eta^2(\mu_2\text{-C,O})]$ site
635.0	616.2	629.6	635.0, 616.2	635.0, 629.6	1.0305	1.0086	$c\text{-La}_2(\mu\text{-C})(\mu\text{-O})$ site
628.6	610.5	623.0	628.6, 610.5	628.7, 623.0	1.0297	1.0090	$c\text{-La}_2(\mu\text{-C})(\mu\text{-O})$
500.2	496.1	477.9	500.2, 496.1	500.2, 477.9	1.0083	1.0467	$c\text{-La}_2(\mu\text{-C})(\mu\text{-O})$
497.4	493.4	475.2	497.4, 493.2	497.3, 475.2	1.0081	1.0467	$c\text{-La}_2(\mu\text{-C})(\mu\text{-O})$ site

1733.8 cm^{-1} with $^{13}C^{16}O$, and to 1731.1 cm^{-1} with $^{12}C^{18}O$. The mixed $^{12}C^{16}O$ + $^{13}C^{16}O$ and $^{12}C^{16}O$ + $^{12}C^{18}O$ isotopic spectra (Figure 3) yield only sums of the corresponding pure isotopic bands, and, hence, are indicative of a monocarbonyl molecule. The isotopic $^{12}C/^{13}C$ and $^{16}O/^{18}O$ ratios are 1.0224 and 1.0240, respectively, also indicating single CO involvement. As can be seen in Figure 1, doping with CCl_4 has no effect on these bands, suggesting that the products are neutral. The band at 1772.7 cm^{-1} is therefore assigned to the C–O stretching vibration of the neutral lanthanum monocarbonyl, LaCO.

The DFT calculations lend strong support to this assignment. The LaCO molecule is predicted to have a linear geometry (Figure 5) with a $^4\Sigma_g^-$ ground state. The ground states of the isomers LaOC and La(μ^2-CO) lie 31.94 and 14.19 kcal mol^{-1} higher in energy than that of the linear LaCO, respectively. This is consistent with previous theoretical investigations.[8] At the BPW91/6–311++G(d,p)-SDD level, the doublet and sextet LaCO are about 5.98 and 126.84 kcal mol^{-1} higher in energy than the quartet ground state of LaCO, respectively. The calculated frequency of the C–O stretching mode of the quartet LaCO species is 1790.8 cm^{-1} (Table 2), showing a very good scale factor (ratio of the observed frequency to the calculated frequency) of 0.9899. Our results are consistent with previous predictions (1844–1778 cm^{-1}) obtained by the DFT method using the gradient and quasi-relativistic corrections, indicating that relativistic effects only slightly influence the vibrational frequencies.[8] Equally importantly, the calculated $^{12}C^{16}O/^{13}C^{16}O$ and $^{12}C^{16}O/^{12}C^{18}O$ isotopic frequency ratios of 1.0230 and 1.0244 are in accordance with the experimental observations, 1.0224 and 1.0240, respectively. This excellent agreement substantiates the identification of the quartet lanthanum monocarbonyl moiety from the matrix IR spectrum. Further discussion about the electron configuration and the bonding characteristics of the LaCO molecule will be given below.

The intensities of the absorption bands at around 1985.0 cm^{-1} (Table 1 and Figure 2) were seen to increase markedly on going to high CO concentrations and low laser powers. Isotopic experiments yielded vibrational-frequency ratios typical of C–O stretching vibrations. In the mixed isotopic experiments (not shown here), complicated bands were observed, which are too difficult to be resolved and are tentatively assigned to the $La(CO)_n$ ($n > 1$) molecules.

$La_2[\eta^2(\mu_2\text{-C,O})]$ and $c\text{-La}_2(\mu\text{-C})(\mu\text{-O})$: Variations in the IR spectra as a function of changes in the CO concentration and laser energy are of particular interest here. With high CO concentration (0.2 %) and low laser energy (4 mJ per pulse), the $La(CO)_n$ molecules

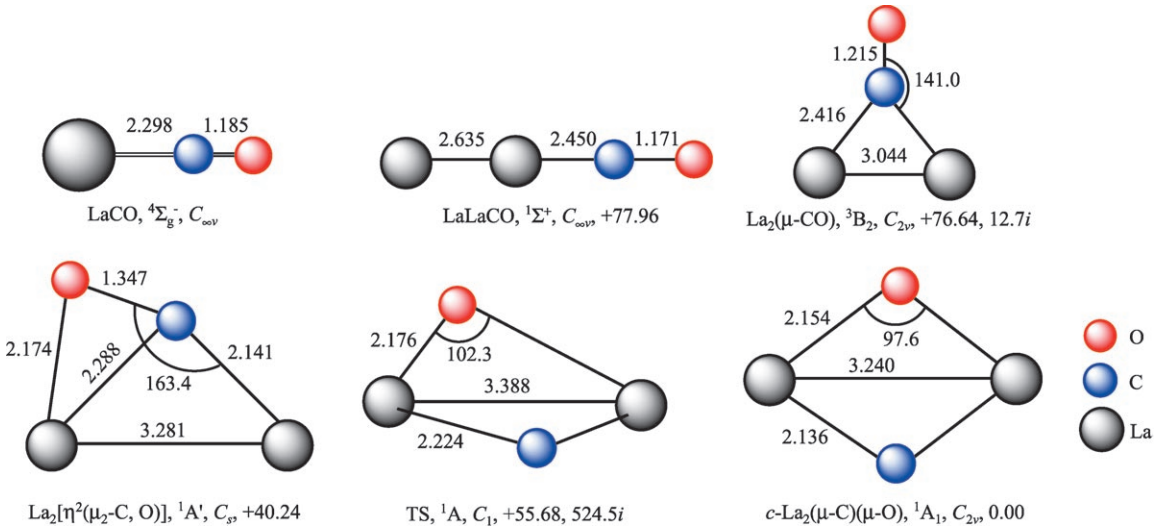

Figure 5. Optimized structures (bond lengths in Angstrom, bond angles in degree), electronic ground states, point groups, and relative energies (in kcal mol^{-1}) of the LaCO and La$_2$CO isomers, calculated at the BPW91/6–311++G(d,p)-SDD level. The letter "*i*" denotes the imaginary frequency (in cm^{-1}). For the transition state (TS), the dihedral angle is 95.7°.

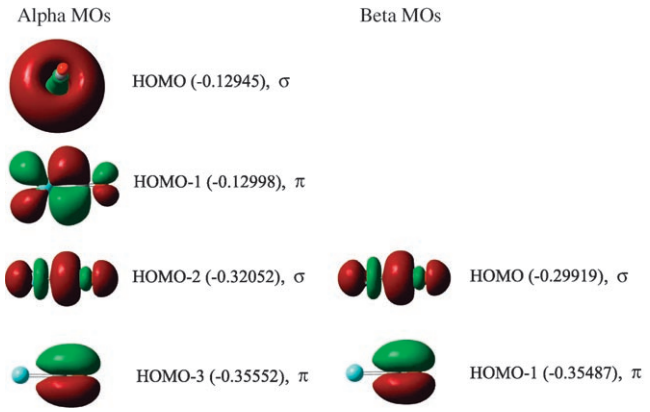

Figure 6. Molecular orbital pictures of quartet LaCO, showing the highest occupied molecular orbitals down to the third valence molecular orbital from the HOMO. The alpha HOMO−1, alpha HOMO−3, and beta HOMO−1 are twofold degenerate; only one of each of the orbital pairs is plotted here. The orbital energies are given in hartree (in parentheses).

are the primary products resulting from sample deposition, as discussed above. New absorption bands were observed following sample annealing with lower CO concentration (0.02 %) and higher laser power (9 mJ per pulse) (Table 1 and Figures 1 and 2). The bands at 1147.9, 1145.9, and 1144.9 cm^{-1} bands disappeared following broad-band irradiation, and did not recover upon further annealing. In contrast, the intensities of new bands at 635.0, 628.6, 500.2, and 497.4 cm^{-1} increased slightly on annealing, increased sharply upon broad-band irradiation at the expense of the 1147.9, 1145.9, and 1144.9 cm^{-1} bands, and increased significantly on further annealing. On the basis of the change in growth/decay characteristics as a function of changes in experimental conditions, the absorptions in the 1160–1130 cm^{-1} region can be collectively assigned to one species and the absorptions in the 650–460 cm^{-1} region assigned to another. Furthermore, the latter species corresponds to an isomer of the former. Note that the new bands were observed only at lower CO concentration and higher laser power than those for mononuclear La carbonyls, indicating that the new products involve more than one La atom. Doping with CCl_4 as an electron scavenger has no effect on these bands, indicating that the products are neutral (Figure 1).

The 1147.9, 1145.9, and 1144.9 cm^{-1} absorptions shifted to 1120.5, 1118.5, and 1117.5 cm^{-1} with $^{13}C^{16}O$, and to 1125.2, 1123.2, and 1122.2 cm^{-1} with $^{12}C^{18}O$, respectively (Table 1), exhibiting isotopic frequency ratios ($^{12}C^{16}O/^{13}C^{16}O$: 1.0245, 1.0245, and 1.0245; $^{12}C^{16}O/^{12}C^{18}O$: 1.0202, 1.0202, and 1.0202) characteristic of C–O stretching vibrations. In the mixed $^{12}C^{16}O+^{13}C^{16}O$ and $^{12}C^{16}O+^{12}C^{18}O$ experiments (Figure 3) only pure isotopic counterparts were observed, indicating that only one CO subunit is involved. In analogy to the Sc$_2$[η^2(μ$_2$-C,O)] molecule,[6] on the basis of the isotopic substitution and the CO concentration and laser power dependences of product yields, the absorptions at 1147.9, 1145.9, and 1144.9 cm^{-1} are assigned to the C–O stretching modes of the La$_2$[η^2(μ$_2$-C,O)] molecule in different matrix sites.

The 635.0 and 628.6 cm^{-1} bands showed very small shifts

Table 2. Comparison of observed and calculated IR frequencies [cm^{-1}] for LaCO, La$_2$[η^2(μ$_2$-C,O)], and *c*-La$_2$(μ-C)(μ-O).

Species	Mode	Observed Freq	Observed $^{12}C/^{13}C$	Observed $^{16}O/^{18}O$	Calculated Freq	Calculated $^{12}C/^{13}C$	Calculated $^{16}O/^{18}O$	Scale Factor (obsd/calcd)
LaCO	ν_{C-O}	1772.7	1.0224	1.0240	1790.8	1.0230	1.0244	0.9899
La$_2$[η^2(μ$_2$-C,O)]	ν_{C-O}	1145.9	1.0245	1.0202	1138.1	1.0255	1.0201	1.0069
c-La$_2$(μ-C)(μ-O)	ν_{La-C}	628.6	1.0297	1.0090	660.6	1.0291	1.0104	0.9516
c-La$_2$(μ-C)(μ-O)	ν_{La-O}	500.2	1.0083	1.0467	482.8	1.0058	1.0487	1.0360

Table 3. The natural bond orbital analysis results of the LaCO molecule calculated at the BPW91/6–311++G(d, p)-SDD level.[a]

				La (%)						C (%)		
bond	spin	type	$100\|C_A\|^2$	s	p	d	f	g	$100\|C_A\|^2$	s	p	d
La–C	α	π	41.61	0.00	0.01	93.60	6.38	0.01	58.39	0.00	99.98	0.02
La–C	α	π	41.61	0.00	0.01	93.60	6.38	0.01	58.39	0.00	99.98	0.02

				C (%)				O (%)		
			$100\|C_A\|^2$	s	p	d	$100\|C_A\|^2$	s	p	d
C–O	α	σ	31.14	30.87	68.97	0.16	68.86	44.00	55.88	0.11
C–O	β	π	29.69	0.00	99.45	0.55	70.31	0.00	99.87	0.13
C–O	β	π	29.69	0.00	99.45	0.55	70.31	0.00	99.87	0.13
C–O	β	σ	31.32	30.73	69.08	0.19	68.68	45.00	54.88	0.13

[a] In the table, C_A is the polarization coefficient.

Table 4. The natural electron configuration of the LaCO molecule calculated at the BPW91/6–311++G(d,p)-SDD level.

Atom	Alpha-spin orbitals	Beta-spin orbitals
La	[core] 6s(0.93) 4f(0.07) 5d(1.02) 5f(0.01)	[core] 6s(0.04) 4f(0.01) 5d(0.04)
C	[core] 2s(0.76) 2p(1.74) 3p(0.04) 4s(0.02)	[core] 2s(0.74) 2p(1.06) 3p(0.01) 4s(0.01)
O	[core] 2s(0.86) 2p(2.53) 3s(0.01) 3p(0.01)	[core] 2s(0.85) 2p(2.22)

with $^{12}C^{18}O$ (5.4 and 5.6 cm^{-1}), but larger shifts with $^{13}C^{16}O$ (18.8 and 12.4 cm^{-1}) were observed. The $^{12}C^{16}O/^{13}C^{16}O$ frequency ratios of 1.0305 and 1.0297 (Table 1) imply that these bands arise from a La–C stretching of the same species in different matrix trapping sites (Figure 4). The 500.2 and 497.4 cm^{-1} bands showed very small shifts with $^{13}C^{16}O$ (4.1 and 4.0 cm^{-1}), but large shifts with $^{12}C^{18}O$ (22.3 and 22.2 cm^{-1}) were observed. The $^{12}C^{16}O/^{12}C^{18}O$ frequency ratios of 1.0467 and 1.0467 indicate that the 500.2 and 497.4 cm^{-1} bands are due to a La–O stretching of the same species in different trapping sites. The mixed isotopic spectra (Figure 4) indicate that only one C and one O atom, which are separated from each other, are involved. As the intensities of these two pairs of bands sharply increased upon broad-band irradiation, at the expense of the $La_2[\eta^2(\mu_2\text{-C,O})]$ molecule, they are assigned to the La–C and La–O stretching vibrations of the C–O dissociated product $c\text{-La}_2(\mu\text{-C})(\mu\text{-O})$ in two trapping sites.

The excellent agreement between experimental and calculated vibrational frequencies, relative absorption intensities, and isotopic shifts, provides compelling evidence for the identification of the $La_2[\eta^2(\mu_2\text{-C,O})]$ and $c\text{-La}_2(\mu\text{-C})(\mu\text{-O})$ molecules. The calculated $^{12}C^{16}O/^{13}C^{16}O$ and $^{12}C^{16}O/^{12}C^{18}O$ frequency ratios for $La_2[\eta^2(\mu_2\text{-C,O})]$ are 1.0255 and 1.0201, respectively, in accordance with the observed values (1.0245 and 1.0202, Table 2). The La–La stretching frequency is predicted to be 121.5 cm^{-1}, which is beyond the present spectral range of 5000–400 cm^{-1}. The La–C and La–O stretching frequencies of $La_2[\eta^2(\mu_2\text{-C,O})]$ are predicted to be 585.9 and 455.2 cm^{-1}, respectively, while their intensities (5 and 32 km mol^{-1}) are too small to be detected. Excellent agreement between the experimental and calculated results was also observed for $c\text{-La}_2(\mu\text{-C})(\mu\text{-O})$ (see Table 2). The identification of the $La_2[\eta^2(\mu_2\text{-C,O})]$ and $c\text{-La}_2(\mu\text{-C})(\mu\text{-O})$ molecules is strongly supported by the scale factors. The scale factors are 1.0069 for the C–O stretching of $La_2[\eta^2(\mu_2\text{-C,O})]$, 0.9516 for the La–C stretching of $c\text{-La}_2(\mu\text{-C})(\mu\text{-O})$, and 1.0360 for the La–O stretching of $c\text{-La}_2(\mu\text{-C})(\mu\text{-O})$.

Our DFT calculations predict that $La_2[\eta^2(\mu_2\text{-C,O})]$ has a $^1A'$ ground state with a La–O bond length of 2.174 Å and two inequivalent La–C bonds of length 2.141 and 2.288 Å in the same plane (Figure 5). The CO group leans toward the two La atoms with ∢La-C-O of 163.4°, which is 8.9° larger than that in $Sc_2[\eta^2(\mu_2\text{-C,O})]$.[6] In contrast, the $\eta^2(\mu_3\text{-C},\mu_2\text{-O})$ ligand in $[Nb_3(\eta^5\text{-}C_5H_5)_3(CO)_7]$ leans toward the Nb(1)–Nb(2) vector, with ∢Nb(3)-C-O of 169.6° and a C–O bond length of 1.303 Å.[15] An analogous Mn-C-N unit with ∢Mn-C-N of 168° is observed in $[Mn_2(\mu\text{-}p\text{-}CH_3C_6H_4NC)Mn_2(Ph_2PCH_2PPh_2)_2(CO)_4]$.[16] $La_2[\eta^2(\mu_2\text{-C,O})]$ has a C–O bond length of 1.347 Å with ν_{C-O} of 1145.9 cm^{-1}. To our knowledge these constitute the longest C–O bond length and lowest ν_{C-O} values for a C–O bond reported so far. In contrast, the C–O bond length and ν_{C-O} values are 1.320 Å and 1193.4 cm^{-1} in $Sc_2[\eta^2(\mu_2\text{-C,O})]$[6] and 1.211 Å and 1613.9 cm^{-1} in $OSc(\eta^2\text{-CO})$,[17] respectively.

Our DFT calculations show that the ground state of $La_2[\eta^2(\mu_2\text{-C,O})]$ lies 40.24 kcal mol^{-1} above that of its most stable C–O dissociated isomer, $c\text{-La}_2(\mu\text{-C})(\mu\text{-O})$. The ground states of the terminal-bonded LaLaCO and bridge-bonded $La_2(\mu\text{-CO})$ isomers are 77.96 and 76.64 kcal mol^{-1} higher than the ground state of $c\text{-La}_2(\mu\text{-C})(\mu\text{-O})$, respectively (Figure 5). The markedly elongated C–O bond (1.347 Å) in $La_2[\eta^2(\mu_2\text{-C,O})]$ is inclined to dissociation. The C–O bond is dissociated in the transition state (TS), in which the dihedral angle is 95.7°. The barrier height for the $La_2[\eta^2(\mu_2\text{-C,O})]$ to $c\text{-La}_2(\mu\text{-C})(\mu\text{-O})$ isomerization (15.45 kcal mol^{-1}) is similar to that for the isomerization of $Sc_2[\eta^2(\mu_2\text{-C,O})]$ to $c\text{-Sc}_2(\mu\text{-C})(\mu\text{-O})$ (15.10 kcal mol^{-1}),[6] which can be attained by UV/Vis irradiation. Anomalous C–O bond weakening has been reported for chemisorbed CO in side-on-bonded modes on transition-metal (model-catalyst) surfaces, for which ν_{C-O} values were observed in the range 1100–1400 cm^{-1}.[18] Interestingly, the observations presented here depict the whole process, starting with the interaction of CO with metal and ending with CO dissociation, as shown in Figure 5. These findings are a key toward explaining the unusually low ν_{C-O} values (1100–1400 cm^{-1}) of the chemisorbed CO molecules on transition-metal surfaces[18] and for understanding the activation process of CO dissociation on metal catalysts.

Bonding mechanism of LaCO: Interestingly, the C–O stretching frequency (1772.7 cm^{-1}) in LaCO, is the lowest observed for a terminal CO in any known neutral MCO molecule, implying an anomalously enhanced metal-to-CO back-bonding in this molecule. Corresponding experiments for Sc and Y yield much higher frequencies (ScCO: 1834.2, YCO: 1874.1 cm^{-1} in solid argon),[19] suggesting that the f-orbital participation in bonding in LaCO is significant. As illustrated in Figure 6, the alpha-spin highest occupied molecular orbital (HOMO) is largely La 6s in character and is nonbonding. It can be seen from the NBO analysis results, reported in Table 3, that the degenerate alpha-spin HOMO−1 orbitals (Figure 6) are of π-type and consist mainly of contributions from the La 5d and 4f, and the C 2p atomic orbitals. The alpha-spin HOMO−2 and HOMO−3 orbitals correspond predominantly to the depressed σ-type and enhanced π-type C–O bonds, respectively, and the corresponding beta-spin molecular orbitals are the same (as shown in Table 3). The NBO analysis results also show that the formation of the $^4\Sigma_g^-$ LaCO ground state, from the La $6s^2 5d^1$ ground electron configuration and CO, involves La 6s→4f promotion (Table 4). This promotion increases the strength of La–CO bonding by decreasing the σ repulsion and significantly increasing the La 5d and 4f→CO 2π back-bonding. The very low electronegativity of La (Pauling scale: 1.10)[20] may account for the observed enhanced π back-bonding and therefore low CO-stretching frequency. The present DFT calculations predict the bonding energy of La with CO to be 41.24 kcal mol^{-1}. This strong interaction is consistent with the observation that broad-band irradiation does not lead to an observable UV-photolysis effect in LaCO.

It can be seen from Table 3 that the $100|C_A|^2$ (C_A is the polarization coefficient) of the La atom in the π-type La–C bond is 41.61%, with contributions from La 6s (0.00), La 6p (0.01%), La 5d (93.60%), La 4f (6.38%), and La 5g (0.01%). Contributions to the La–C bond from C 2s, C 2p, and C 3d of 0.00, 99.98, and 0.02%, respectively, suggest that the formation of the La–C bond is primarily from contributions from the La 5d, La 4f, and C 2p orbitals. This is in accordance with previous calculations, which take relativistic effects into account.[8] It is also found that the interaction of the C 2s, C 2p, O 2s, and O 2p orbitals plays a major role in the σ-type C–O bond, whereas the interaction of the C 2p and O 2p orbitals is more important in the π-type C–O bond (Table 3).

The unusually low C–O stretching frequency in LaCO (ν_{C-O} = 1772.7 cm^{-1}) is reminiscent of ThCO,[4] a molecule that exhibits a slightly higher C–O stretching frequency at 1817.5 cm^{-1}. It was predicted that ThCO has a $^3\Sigma^-$ ground state, with two metal-based electrons occupying the nonbonding 6σ molecular orbital, which is largely Th 7s in character, and the remaining two occupying the doubly degenerate 3π molecular orbital, which comprises the Th 6d→CO 2π back-bonding.[4] It may be concluded that the degree of metal-to-CO back-bonding in LaCO is larger than that in ThCO, and much larger than that in any other known neutral MCO molecule.

Conclusion

The reactions of laser-ablated lanthanum atoms with CO molecules in solid argon at 7 K have been investigated. The IR absorption band at 1772.7 cm^{-1} is assigned to the C–O stretching mode of the LaCO molecule, and the absorption at 1145.9 cm^{-1} to the side-on-bonded $La_2[\eta^2(\mu_2\text{-C,O})]$ molecule. This CO-activated $La_2[\eta^2(\mu_2\text{-C,O})]$ molecule undergoes UV/Vis-photoinduced rearrangement to the CO-dissociated molecule, *c*-$La_2(\mu\text{-C})(\mu\text{-O})$. DFT calculations have been performed on these molecules and lend strong support to the experimental assignments of the IR spectra. It is predicted that LaCO is a linear molecule with a quartet ground state; its formation involves La 6s→4f promotion. This promotion increases the strength of La–CO bonding by decreasing the σ repulsion and anomalously increasing the La 5d and 4f→CO 2π back-bonding, which accounts for the unusually low C–O stretching frequency in LaCO (ν_{C-O} = 1772.7 cm^{-1}). The present findings are a key toward explaining the unusually low ν_{C-O} values (1100–1400 cm^{-1}) of the chemisorbed CO molecules on transition-metal surfaces and for understanding the activation process for CO dissociation on metal catalysts.

Acknowledgements

We thank Prof. Mingfei Zhou for helpful discussions and a reviewer for valuable suggestions. This work was supported by a Grant in Aid for Scientific Research (B; Grant No. 17350012) from the Ministry of Education, Culture, Sports, Science and Technology (MEXT) of Japan, and by Marubun Research Promotion Foundation. L.J. thanks the MEXT of Japan and Kobe University for the Honors Scholarship.

[1] F. A. Cotton, G. Wilkinson, C. A. Murillo, M. Bochmann, *Advanced Inorganic Chemistry*, 6th ed., Wiley, New York, **1999**.
[2] S. P. Walsh, W. A. Goddard, *J. Am. Chem. Soc.* **1976**, *98*, 7908.
[3] a) M. F. Zhou, L. Andrews, C. W. Bauschlicher, Jr., *Chem. Rev.* **2001**, *101*, 1931; b) H. J. Himmel, A. J. Downs, T. M. Greene, *Chem. Rev.* **2002**, *102*, 4191, and references therein.
[4] a) M. F. Zhou, L. Andrews, J. Li, B. E. Bursten, *J. Am. Chem. Soc.* **1999**, *121*, 12188; b) J. Li, B. E. Bursten, M. F. Zhou, L. Andrews, *Inorg. Chem.* **2001**, *40*, 5448.
[5] E. L. Muetterties, J. Stein, *Chem. Rev.* **1979**, *79*, 479.
[6] L. Jiang, Q. Xu, *J. Am. Chem. Soc.* **2005**, *127*, 42.
[7] See, for example: a) C. Xu, L. Manceron, J. P. Perchard, *J. Chem. Soc. Faraday Trans.* **1993**, *89*, 1291; b) V. E. Bondybey, A. M. Smith, J. Agreiter, *Chem. Rev.* **1996**, *96*, 2113; c) S. Fedrigo, T. L. Haslett, M. Moskovits, *J. Am. Chem. Soc.* **1996**, *118*, 5083; d) L. Khriachtchev, M. Pettersson, N. Runeberg, J. Lundell, M. Rasanen, *Nature* **2000**, *406*, 874; e) H. J. Himmel, L. Manceron, A. J. Downs, P. Pullumbi, *J. Am. Chem. Soc.* **2002**, *124*, 4448; f) J. Li, B. E. Bursten, B. Y. Liang, L. Andrews, *Science* **2002**, *295*, 2242; g) L. Andrews, X. F. Wang, *Science* **2003**, *299*, 2049.
[8] G. Hong, X. Lin, L. Li, G. Xu, *J. Phys. Chem. A* **1997**, *101*, 9314.
[9] T. R. Burkholder, L. Andrews, *J. Chem. Phys.* **1991**, *95*, 8697.
[10] a) M. F. Zhou, N. Tsumori, L. Andrews, Q. Xu, *J. Phys. Chem. A* **2003**, *107*, 2458; b) L. Jiang, Q. Xu, *J. Chem. Phys.* **2005**, *122*, 034505.
[11] Gaussian 03, Revision B.04, M. J. Frisch, G. W. Trucks, H. B. Schlegel, G. E. Scuseria, M. A. Robb, J. R. Cheeseman, J. A. Montgomery, Jr., T. Vreven, K. N. Kudin, J. C. Burant, J. M. Millam, S. S. Iyengar,

J. Tomasi, V. Barone, B. Mennucci, M. Cossi, G. Scalmani, N. Rega, G. A. Petersson, H. Nakatsuji, M. Hada, M. Ehara, K. Toyota, R. Fukuda, J. Hasegawa, M. Ishida, T. Nakajima, Y. Honda, O. Kitao, H. Nakai, M. Klene, X. Li, J. E. Knox, H. P. Hratchian, J. B. Cross, C. Adamo, J. Jaramillo, R. Gomperts, R. E. Stratmann, O. Yazyev, A. J. Austin, R. Cammi, C. Pomelli, J. W. Ochterski, P. Y. Ayala, K. Morokuma, G. A. Voth, P. Salvador, J. J. Dannenberg, V. G. Zakrzewski, S. Dapprich, A. D. Daniels, M. C. Strain, O. Farkas, D. K. Malick, A. D. Rabuck, K. Raghavachari, J. B. Foresman, J. V. Ortiz, Q. Cui, A. G. Baboul, S. Clifford, J. Cioslowski, B. B. Stefanov, G. Liu, A. Liashenko, P. Piskorz, I. Komaromi, R. L. Martin, D. J. Fox, T. Keith, M. A. Al-Laham, C. Y. Peng, A. Nanayakkara, M. Challacombe, P. M. W. Gill, B. Johnson, W. Chen, M. W. Wong, C. Gonzalez, J. A. Pople, Gaussian, Inc., Pittsburgh PA, **2003**.

[12] a) A. D. Becke, *Phys. Rev. A* **1988**, *38*, 3098; b) J. P. Perdew, K. Burke, Y. Wang, *Phys. Rev. B* **1996**, *54*, 16533.

[13] a) M. J. Frisch, J. A. Pople, J. S. Binkley, *J. Chem. Phys.* **1984**, *80*, 3265; b) D. Andrae, U. Haussermann, M. Dolg, H. Stoll, H. Preuss, *Theor. Chim. Acta* **1990**, *77*, 123.

[14] E. D. Glendening, A. E. Reed, J. E. Carpenter, F. Weinhold, NBO, version 3.1.

[15] W. A. Herrmann, H. Biersack, M. L. Ziegler, K. Weidenhammer, R. Siegel, D. Rehder, *J. Am. Chem. Soc.* **1981**, *103*, 1692.

[16] L. S. Benner, M. M. Olmstead, A. L. Balch, *J. Organomet. Chem.* **1978**, *159*, 289.

[17] M. F. Zhou, L. Andrews, *J. Am. Chem. Soc.* **1998**, *120*, 13230.

[18] a) D. W. Moon, S. L. Bernasek, D. J. Dwyer, J. L. Gland, *J. Am. Chem. Soc.* **1985**, *107*, 4363; b) N. D. Sinn, T. E. Madey, *Phys. Rev. Lett.* **1984**, *53*, 2481; c) F. M. Hoffmann, R. A. de Paola, *Phys. Rev. Lett.* **1984**, *52*, 1697.

[19] M. F. Zhou, L. Andrews, *J. Phys. Chem. A* **1999**, *103*, 2964.

[20] *CRC Handbook of Chemistry and Physics*, 79th ed. (Ed.: D. R. Lide), CRC, Boca Raton, FL, **1998**, pp. 9–74.

Received: August 23, 2005
Published online: February 3, 2006

